Med Biol Eng Comput (2013) 51:135–142
DOI 10.1007/s11517-012-0977-6

ORIGINAL ARTICLE

Remote sensing of patterns of cardiac activity on an ambulatory subject using millimeter-wave interferometry and statistical methods

Ilya V. Mikhelson · Sasan Bakhtiari · Thomas W. Elmer II · Alan V. Sahakian

Received: 10 May 2012 / Accepted: 11 October 2012 / Published online: 26 October 2012

Abstract Using a 94-GHz millimeter-wave interferometer, we are able to calculate the relative displacement of an object. When aimed at the chest of a human subject, we measure the minute motions of the chest due to cardiac activity. After processing the data using a wavelet multiresolution decomposition, we are able to obtain a signal with peaks at heartbeat temporal locations. In order for these heartbeat temporal locations to be accurate, the reflected signal must not be very noisy. Since there is noise in all but the most ideal conditions, we created a statistical algorithm in order to compensate for unconfident temporal locations as computed by the wavelet transform. By analyzing the statistics of the peak locations, we fill in missing heartbeat temporal locations and eliminate superfluous ones. Along with this, we adapt the processing procedure to the current signal, as opposed to using the same method for all signals. With this method, we are able to find the heart rate of ambulatory subjects without any physical contact.

I. V. Mikhelson
Electrical Engineering and Computer Science,
Northwestern University, Evanston, IL 60208, USA
e-mail: i-mikhelson@u.northwestern.edu

S. Bakhtiari · T. W. Elmer II
Nuclear Engineering Division,
Argonne National Laboratory, Argonne, IL 60439, USA
e-mail: bakhtiari@anl.gov

T. W. Elmer II
e-mail: elmer@anl.gov

A. V. Sahakian (✉)
Electrical Engineering and Computer Science/Biomedical Engineering, Northwestern University, Evanston,
IL 60208, USA
e-mail: sahakian@eecs.northwestern.edu

Keywords Remote sensing · Millimeter-wave · Heartbeat detection · Heart rate · Wavelets

1 Introduction

There are many reasons to gather physiological measurements at a distance without any physical contact. These include medical monitoring, security, and life detection. Whether in a hospital or at a subject's home, non-contact monitoring is a non-obtrusive and safe way to monitor a patient without interfering with his/her life. In addition, during lengthy tests, such as for sleep apnea, the subject can be uncomfortable wearing monitoring equipment. For this purpose, it has been demonstrated that non-contact equipment can be used for respiratory function observations while a person sleeps [17]. Another very useful application is for detection of lying. In this scenario, a person answers questions while vital signs are monitored without the subject's knowledge [4]. In addition, such technology has been used to find whether people are alive in situations where it may be dangerous to retrieve a person [7].

In order to obtain vital signs, a popular approach has been to look at the displacement of the chest wall and to isolate displacements due to cardiac activity and respiration. In the 1970s and 1980s, Lin [6] showed that the respiratory and cardiac rates could be gathered from a clothed subject at a distance of roughly 0.3 m. These early studies used the Doppler effect to calculate physiological parameter measurements. Since the radio frequency waves undergo a frequency shift upon reflection from a moving surface (in this case the chest), the change in frequency between the transmitted and reflected signals can be analyzed to find the velocity of the chest wall, and subsequently the heart rate and respiratory rate.

A more accurate method is to gather in-phase and quadrature reflections from the subject's chest in order to find the phase of the reflected signal [8, 10–12, 14]. The displacement modulates the phase, so the displacement can be found directly after some further processing. The main difference in every approach has been how to extract the tiny motions due to cardiac activity from the entire displacement signal.

A common approach has been to take a Fourier transform of the displacement signal. This approach works well if the signal is stationary and if the subject is nearly motionless. In the Fourier domain, there is a peak at the breathing frequency and a peak at the heart rate frequency. However, even without movement, the peak from respiration can obscure that from cardiac activity. When gross body movement occurs, both peaks can be easily lost in the large low frequency peak that movement creates.

More realistically, the heart and respiratory rates cannot be assumed to be stationary, since no individual breathes perfectly uniformly for each breath and there is an inherent arrhythmia in the cardiac pattern of all healthy people. Therefore, an analysis involving time and frequency [1] becomes a more appealing approach.

In previous research [5, 10], wavelets have been used to decompose the displacement signal. Wavelets provide excellent time resolution for rapid events in time, such as heartbeats, and good frequency resolution for slower events in time, such as breathing [16]. However, wavelets alone cannot always find every heartbeat. Therefore, statistical methods lend themselves nicely to enhance this application. The rest of this paper will discuss a statistical method to find cardiac rhythm as accurately as possible.

2 Methods

2.1 Pre-processing

To find heart rate, we first gather a chest displacement signal, i.e., the movement of the chest perpendicular to the frontal plane. To obtain a chest displacement signal, we used a 94-GHz continuous-wave millimeter-wave interferometer [2] and a National Instruments USB-9239 24-bit analog-to-digital converter with a sampling rate of 5,000 Hz to collect in-phase (I) and quadrature (Q) components of the reflection. Details of the system can be found in [10]. All processing was performed in MATLAB [9].

The received reflection from the millimeter-wave signal, when aimed at the chest, is a combination of several vector components [11, 10]. These components include reflections from stationary or moving objects not related to the subject. The vector component due to chest wall motion can be isolated using circle-fitting in the in-phase–quadrature space. Then, using simplifying assumptions about noise and interference, the reflection received by the antenna due to chest motion can be used to find the chest displacement signal given by:

$$\text{Displacement} = \frac{\lambda_0}{4\pi} \times \text{unwrap}\left[\arctan\left(\frac{Q}{I}\right)\right], \quad (1)$$

where $\lambda_0 = \frac{2\pi c}{\omega_0}$, c is the speed of light, ω_0 is the angular frequency $94 \times 2\pi \times 10^9$ rads/s, and "unwrap" indicates phase unwrapping to account for phase discontinuities at $\pm\pi$ [9, 10].

Then, the displacement waveform is downsampled to 50 Hz and a one-level multi-resolution decomposition is performed on the signal using a symlet 32 wavelet. The detail signal (i.e. the high-pass portion of the decomposition) is then used for further processing. First, we take the absolute value of the detail signal, and then pass it through a moving-average filter of length 20. The entire pre-processing can be seen in Fig. 1. This creates a signal with peaks of varying amplitudes at most of the heartbeat temporal locations [10]. To confirm all processing techniques, an electrocardiogram was gathered concurrently with the data in order to know where the actual heartbeats are present.

2.2 Statistical processing

Since the heights of the peaks generated by the wavelet decomposition vary greatly, and not all peaks are due to heartbeats, and not all heartbeats have a corresponding peak, statistical techniques are used to deal with the variations.

The main idea is to analyze the pre-processed signal in overlapping windows and to adapt the selection criteria for a given peak based on the statistics in that window. The statistical method that is used in each window is the generalized likelihood ratio test (GLRT) [15]. This test compares two statistical distributions and characterizes a given value as belonging to one or the other based on a threshold.

The pre-processed data X are a sequence of discrete values in the set of real numbers ($X \in \mathbb{R}$). For our tests, we

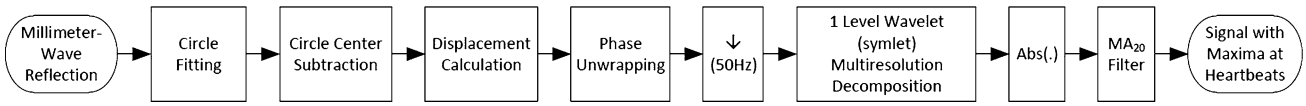

Fig. 1 Pre-processing flowchart, where *downarrow* downsampling, $Abs(\cdot)$ absolute value operator, and MA_{20} 20-point moving-average filter

postulated that X can belong to one of two probability distributions:

heartbeat not present: $f_0(x)$
heartbeat present: $f_1(x)$,

which means that the two hypotheses for the likelihood test are:

$H_0 : X$ is distributed as $f_0(x)$
$H_1 : X$ is distributed as $f_1(x)$.

If $X = x$ is observed, the likelihood ratio test statistic is:

$$L(x) = \frac{f_0(x)}{f_1(x)}, \quad x \in \mathbb{R}.$$

If $L(x) > 1$, then we choose H_0, and if $L(x) < 1$, then we choose H_1.

Using this framework, we analyze the signal by parts. First, a window of the pre-processed signal is selected. Then, all of the maxima are found. We assume, with no other knowledge, that all maxima correspond to heartbeats. "Heartbeat" (HB) values are selected as those points that are within 1/4 of the distance from a peak to the previous peak and within 1/4 of the distance from the same peak to the next peak; "non-heartbeat" (nHB) values are selected as all the rest of the points. This process is illustrated in Fig. 2a.

Then, a probability density function is fitted to the data for both HB and nHB values. For the density function, we chose the log-normal distribution:

$$f(x) = \frac{1}{x\sqrt{2\pi\sigma^2}} e^{-\frac{[\ln(x)-\mu]^2}{2\sigma^2}}.$$

We selected this distribution because our data are always positive (due to the absolute value operation in the pre-processing) and because a normal fit was good in general, as shown in Fig. 2b. We did not want to use a nonparametric distribution in order to not give emphasis to outlying values, but rather to concentrate on the values around the mean of the distribution, and also to create a smooth fit with only one intersection.

Then, we find the first intersection of the distributions. This value is used to determine the threshold for deciding whether a given value belongs to HB or nHB:

$$L(x) = \frac{f_0(x)}{f_1(x)} \underset{H_1}{\overset{H_0}{\gtrless}} \alpha \tag{2}$$

where α is a scaling of the threshold, where the optimal value is determined through experiment.

Using this threshold, we keep only the peaks in the pre-processed signal that are greater in value than the threshold. We also eliminate peaks that have a spacing of less than 0.3 s in order to eliminate heartbeats faster than 200 beats per minute (bpm), since that is above the maximum

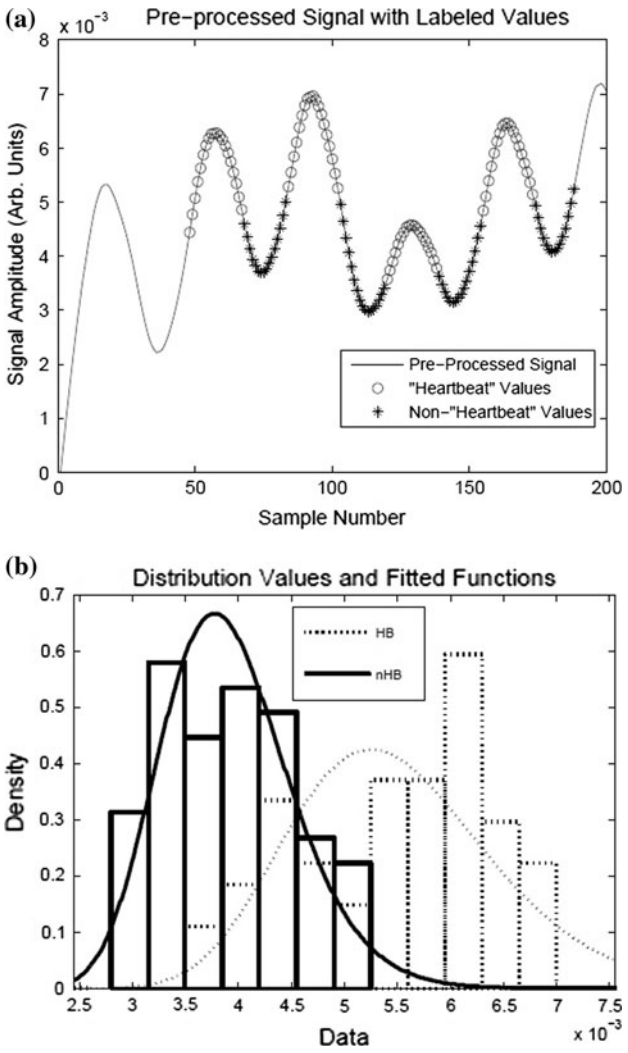

Fig. 2 Statistical data. **a** Initial heartbeat and non-heartbeat selection. **b** Histogram of HB and nHB values and fitted log-normal distributions

for people over 20 years of age according to the conventional formula: max heart rate = 220 − age.

This process is done for the whole signal in overlapping sliding windows. At the end, all of the maxima of the pre-processed signal that are above the threshold and slower than 200 bpm in their respective windows are concatenated. After this, the entire signal is once again checked for heartbeats that are faster than 200 bpm, since the concatenation process might place heartbeats too close together due to the overlapping windows.

Then, we eliminate heartbeats that are too close together as compared to the rest of the heartbeats in the signal. To do this, we find the average spacing of the heartbeats (dAvg), and eliminate those that are closer together than $\gamma \times$dAvg. We also eliminate heartbeats that are too far apart as compared to the rest of the heartbeats in the signal. We once again use dAvg and eliminate those that were farther

apart than $\delta\times$dAvg. The factors γ and δ are found experimentally as most often eliminating false positive detections. Here, γ is a factor to eliminate fast heartbeats, which could be caused by noise, and δ is a factor to eliminate heartbeats in long intervals, since a long interval without heartbeats indicates an unclean, highly nonstationary signal, which is prone to error. The reasoning for performing these pruning steps is that we want to keep only heartbeats that look very much like real heartbeats, thus eliminating as many false positives as possible. The remaining heartbeats belong to the set of *confident heartbeats* (c-HB).

After pruning, we add heartbeats back in based on the spacing in c-HB. If the spacing between any heartbeats in c-HB is greater than $\delta\times$dAvg after pruning, we add in equidistantly spaced points based on the spacing of the heartbeats in c-HB.

Finally, we find a new dAvg for the new c-HB, go through the heartbeats and again prune heartbeats that are too close together based on dAvg. Then, we again add in heartbeats in large intervals based on dAvg. This process is repeated three times to get to the final heartbeat temporal locations (f-HB).

2.3 Filter length optimization

The moving-average filter was chosen to have a length of 400 ms, based on an average, calm, adult human's heart rate. If the heart rate is higher, the moving-average filter might blur together multiple heartbeats. If the heart rate is lower, the moving-average filter might create multiple peaks at each heartbeat. Therefore, it becomes necessary to use an adaptive length for the moving-average filter.

Since there is no prior knowledge of the heart rate, the adaptation has to be based entirely on the pre-processed signal. Since each peak corresponds to a heartbeat, there are also constraint equations corresponding to maximum and minimum heart rate. The equations for this process are presented here, and explained below:

$$s = \text{Pre-processed signal} \tag{3}$$

$$s_d = \frac{\mathrm{d}s}{\mathrm{d}t} \tag{4}$$

$$d = \frac{1}{N-1}\sum_{i=2}^{N}\left(l_i^s - l_{i-1}^s\right) \tag{5}$$

$$h = \frac{1}{N}\sum_{i=1}^{N}\left(p_i^s\right) - \frac{1}{M}\sum_{i=1}^{M}\left(v_i^s\right) \tag{6}$$

$$h_d = \frac{1}{N_d}\sum_{i=1}^{N_d}\left(p_i^{s_d}\right) - \frac{1}{M_d}\sum_{i=1}^{M_d}\left(v_i^{s_d}\right), \tag{7}$$

where N is the number of peaks in s, M is the number of valleys in s, l_i^s is the ith peak location in s, p_i^s is the ith peak value in s, and v_i^s is the ith valley value in s. All of the variables are functions of L_{ma}, the length of the moving-average filter, since the length of the filter determines the peak and valley locations in s.

Using Eqs. (3)–(7), the optimization problem can be formulated as:

$$L_{\text{ma}}^* = \arg\min_{L_{\text{ma}}} \quad L_{\text{ma}} + N + N_d - h - h_d \tag{8}$$

$$s.t. \quad d > 15, \quad L_{\text{ma}} < 75, \quad L_{\text{ma}} > 0. \tag{9}$$

For the optimization, we try to make the peaks as distinct as possible. To do that, we maximize the difference between the peak and valley heights [Eq. (6)] while also minimizing the length of the filter [Eq. (8)] to get as many distinct peaks as possible. At the same time, we also maximize the difference between the peak and valley heights of the derivative of the pre-processed signal [Eq. (7)] in order to get as smooth a signal as possible. In addition, we minimize the number of peaks of the signal and its derivative [Eq. (8)] in order to prevent the filter length from getting too small. The optimization is further constrained to create a heart rate between 40 and 200 bpm. At a sampling rate of 50 Hz, this corresponds to the distance between adjacent peaks [Eq. (5)] being greater than 15 samples and the length of the moving-average filter being less than 75 samples [Eq. (9)]. Solving Eqs. (8) and (9) gives the optimum length of the moving average filter, L_{ma}^*, for the given dataset.

2.4 Result verification

In order to get a consistent measure of the performance of the algorithm, we created a verification algorithm. First, we find the QRS complexes in the concurrently-gathered ECG using the Pan–Tompkins algorithm [13] (*HB* in Fig. 3). Then, each QRS complex temporal location is offset by 0.16 s, an empirically-determined value to account for the time between the QRS-complex and the propagation of the heart motion to the chest wall (oQRS in Fig. 3). Next, each calculated heartbeat temporal location is compared to the offset QRS complex temporal locations. If a heartbeat falls within 0.4 s of the offset QRS complex, it is counted as a true positive (TP); otherwise, it is counted as a false positive (FP). If there is no calculated heartbeat within 0.4 s of the offset QRS complex, it is counted as a false negative (FN). True negatives (TN) do not apply to this data, as we are only interested in finding heartbeats, not their absence. The whole process can be seen in Fig. 3.

Using these measures, we are able to find the recall (or sensitivity) as

$$\text{Recall} = \text{TP}/(\text{TP} + \text{FN}) \tag{10}$$

and precision as

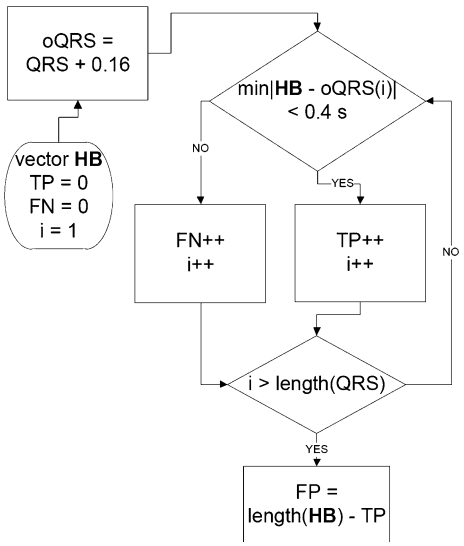

Fig. 3 *Flowchart* of verification algorithm

$$\text{Precision} = \text{TP}/(\text{TP} + \text{FP}). \quad (11)$$

These measures are good indications as to the accuracy of the algorithm, as they not only take the heart rate into account, but also the actual heartbeat temporal locations. If we were to simply use the average of the inter-beat spacings to calculate the heart rate, a lot of false positives followed by a lot of false negatives might give an accurate heart rate, since large spacings and small spacings average out to normal spacings. However, using this verification algorithm, only accurately placed heartbeats contribute to the true positive count.

3 Results

For testing the methods, we received approval from Northwestern University's Office for the Protection of Research Subjects (IRB Project Number: STU00051704). We first tested the statistical algorithm on data gathered from 5 m away with the subject sitting in a chair and breathing normally.

Figure 4a shows the resulting heartbeat temporal locations as calculated by our algorithm. This shows a recall of 100 % and a precision of 100 %. The previous, non-statistical algorithm [10], also calculated the heartbeats with good accuracy for this sample (not shown here). At 8 m away, the previous algorithm [10] had trouble. However, the new algorithm was able to place heartbeats accurately, as shown in Fig. 4b. This is because the data were noisy, which affected the peaks created by the wavelet transform during pre-processing. Since the previous algorithm relies solely on those peaks, it could not place the heartbeats accurately. However, the new method used the statistics of the peaks to find most missing heartbeat temporal locations with a recall of 92.3 % and a precision of 100 %.

The most important result, however, was the ability of the algorithm to process data of a moving subject. In most previous research on this topic, the subject was required to sit against a chair back or stand against a wall to minimize extraneous motions, which would overshadow the motions of the chest due to cardiac activity. In [11], the subject was allowed to move, but reliable heart rate extraction was not able to be performed. With this algorithm, we were able to process data on a slowly moving subject (up to 15 cm/s) with movement toward and away from the antenna and also from side to side.

The displacement of the chest wall due to cardiac activity is on the order of 0.1 mm, while that due to

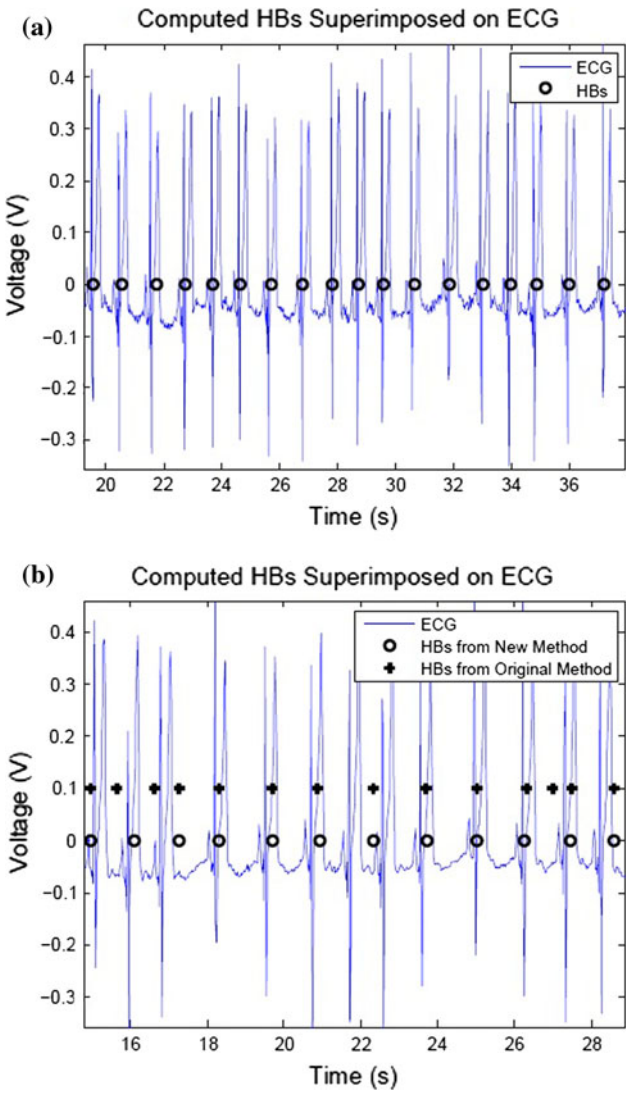

Fig. 4 ECG with superimposed heartbeats gathered at **a** 5 m with breathing using the new method, and **b** 8 m with breathing using both the new method and the original, non-statistical method

respiration varies from approximately 4 to 12 mm [3]. The movement that we processed was more than 1 m, which is thousands of times greater than that due to a heartbeat.

For our tests, we had five subjects. Their characteristics can be seen in Table 1. They all followed the same protocol, described as follows. Starting out seated 3.5 m from the sensor for about 15 s, the subject then stood up and walked slowly toward the sensor until 2 m away. After that, the subject moved backward until 4 m from the sensor, and remained at that distance for about 40 s. Finally, the subject walked more quickly to a distance of 2 m from the sensor.

As mentioned previously, the movements of the subject are much larger than the movements of the chest due to cardiac activity. To find the temporal locations of the heartbeats, we used the algorithms described above with a sliding window length of 4 s and an overlap of 2 s. In order to test the efficacy of the algorithm, we performed a leave-one-out cross validation. First, we created a precision–recall curve (similar to the *receiver operating characteristic* [ROC] curve in detection theory) by varying α, γ, and δ (Sect. 2.2) for four out of the five subjects, an example of which is shown in Fig. 5a. As can be seen, the precision–recall curve passes close to the top right corner, which is a very good indicator of an accurate algorithm. We chose the operating point as being farthest from the origin, and used the corresponding values of α, γ, and δ to test the last subject. This was performed five times, leaving each of the subjects out. In addition, this same kind of analysis was performed for data with no movement, where the subjects sat at distances of 2–9 m in increments of 1 m while either breathing or holding their breath. A sample precision–recall curve for that data can be seen in Fig. 5b.

We then used the verification algorithm to check the results. Table 2 shows the number of true positives, false positives, false negatives, recall, and precision for each of the five subjects, along with the totals. In the state column, m means the subject is moving, nm means the subject is not moving, b means he/she is breathing, and nb means he/she is not breathing.

Table 1 Description of subjects

Subject #	Gender	Age	Height (cm)	BMI
1	F	20	164	18.3
2	M	24	180	26.5
3	M	25	173	22.8
4	M	26	168	20.2
5	M	57	173	25.5

4 Discussion

As seen in Fig. 5, the algorithm performs well at the chosen operating point. As expected, the curve in Fig. 5b passes closer to the top right corner than the curve in Fig. 5a, because the data with movement are harder to process than the data without movement.

There are some uncommon characteristics of the curve for the data without movement, in that it has some abnormally low precision values for specific recall values, most notably when recall is approximately 0.7. This is due to the various pruning and adding steps that were performed in the algorithm, making the error rate a non-monotonic function of the thresholds. However, this does not hinder the algorithm, since the operating point is chosen at a higher recall, where the precision is also higher.

In the presence of movement, the recall tends to be higher than the precision because the algorithm interpolates erroneous heartbeats, as there are not as many "confident" heartbeats in the presence of large movements, as could be expected. Subject 3 had a large number of false negatives because the heartbeats were not placed close enough to the

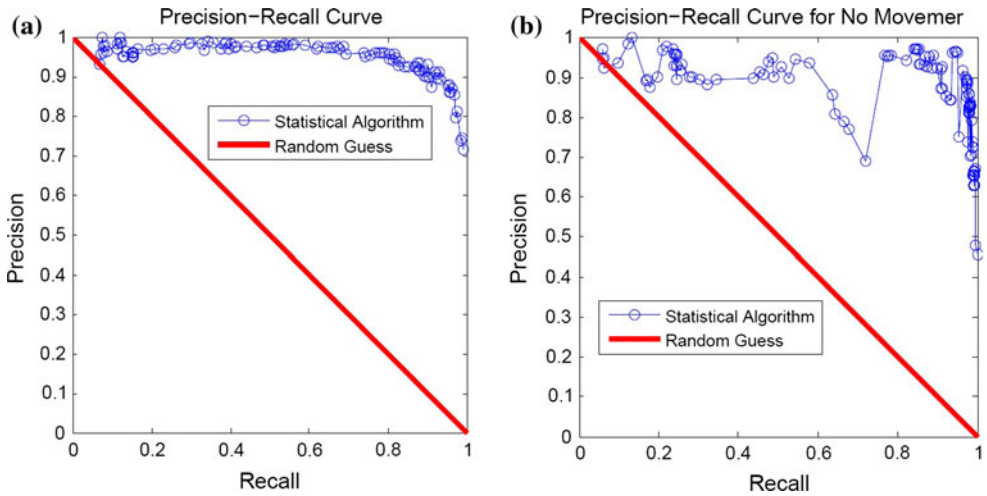

Fig. 5 Precision–recall curves for **a** movement data, and **b** data with no movement

Table 2 Results of proposed algorithm

Subj.	State	TP	FP	FN	Rec (%)	Prec (%)
1	m, b	108	18	5	95.6	85.7
2	m, b	134	16	5	96.4	89.3
3	m, b	275	4	53	83.8	98.6
4	m, b	176	24	4	97.8	88.0
5	m, b	145	16	10	93.6	90.1
1	nm, nb	256	25	39	86.8	91.1
2	nm, nb	367	8	9	97.6	97.9
3	nm, nb	373	27	24	94.0	93.3
4	nm, nb	285	47	11	96.3	85.8
5	nm, nb	370	22	12	96.9	94.4
1	nm, b	272	45	23	92.2	85.8
2	nm, b	323	24	34	90.5	93.1
3	nm, b	351	26	44	88.9	93.1
4	nm, b	265	11	28	90.4	96.0
5	nm, b	368	17	14	96.3	95.6
Total	m, b	838	78	77	91.6	91.5
Total	nm, nb	1,651	129	95	94.6	92.8
Total	nm, b	1,579	123	143	91.7	92.8
All	N/A	4,068	330	315	92.8	92.5

"true" heartbeat temporal locations because they were interpolated over a large area of "unconfident" heartbeats. It is therefore important to notice that the verification is strictly on heartbeat temporal locations, as opposed to rhythm.

The spread of heartbeat temporal locations as detected by our algorithm can be seen in Fig. 6. As expected, when the subject is stationary, the heartbeat temporal locations are very consistent (as was shown in Fig. 4a, b). When there is movement, however, the detection is still very good, but the spread of temporal locations is greater. Although there is a consistent drop-off of discrepancy, these measurements are still not accurate enough for medical metrics such as heart rate variability, which requires very accurate inter-beat times. This is something that we are further researching in two ways: improving the localization of "confident" heartbeats, and increasing the complexity of the statistical algorithm. The former improvement requires better processing algorithms. The latter improvement requires taking more information into account, such as higher moments of the distributions (as opposed to just looking at the first moment as it is now).

When using our algorithm, the parameters that could be adjusted are the size of the moving window, and the

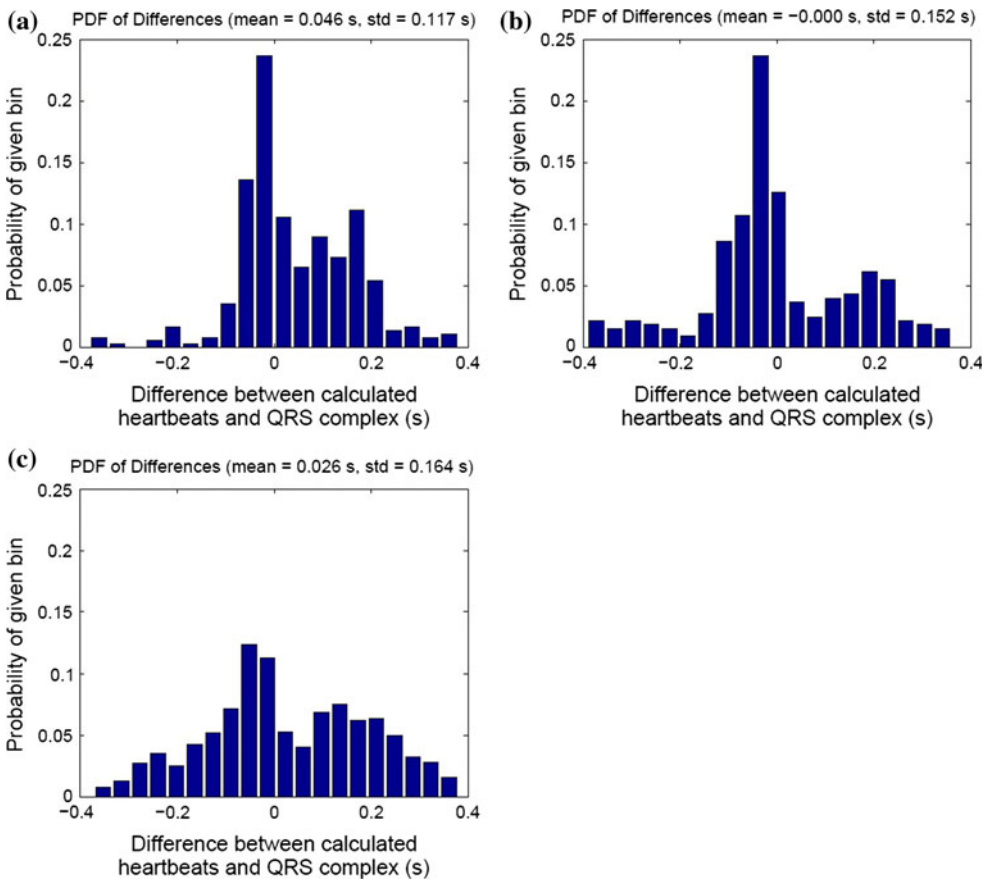

Fig. 6 Probability mass histogram of differences between calculated heartbeat temporal locations and "true" heartbeat temporal locations when **a** the subject is suppressing breathing, **b** the subject is breathing normally, and **c** the subject is breathing normally and moving

overlap between adjacent windows. We empirically chose a window length of 4 s with an overlap of 2 s. A 4-s window is small enough to factor in the statistics of local phenomena, such as respiratory sinus arrhythmia, but also large enough to build up statistics to separate "confident" heartbeats from "unconfident" ones. The overlap of 2 s ensured that we did not miss any heartbeats that may have been "unconfident" compared to the neighboring beats on one side but "confident" compared to beats on the other side.

The statistical algorithm represents an improvement over the method in [10] because it looks at the statistics of the signal as opposed to finding peaks of the pre-processed signal blindly. Although not all heartbeats are detected, the placement of inter-peak heartbeats is accurate for the most part. Some heartbeat temporal locations are more difficult to predict given phenomena such as respiratory sinus arrhythmia, which creates a non-uniform spacing and can cause problems if there are no "confident" heartbeats for a long enough period of time.

Most importantly, we have presented an algorithm that works on moving subjects. This has not been previously done to the authors' knowledge. Future work will focus on more consistent heartbeat temporal location calculations.

It should be noted that this procedure works only for healthy adults. For subjects exhibiting intermittent long inter-beat intervals, this method would add in heartbeats in the large intervals and create a healthy-looking output. Also, young subjects might have a heart rate faster than 200 bpm, in which case the algorithm would prune heartbeats in order to enforce a rate under 200 bpm. However, although this algorithm may not be ready for medical diagnostics, it would perform well in a security setting where the important characteristic is the subject's average heart rate.

This algorithm, though used in post-processing here, can be readily adapted to real-time processing. The average time to run this algorithm over an 8-s window was 0.2564 s (computed as the average time of 100 runs) on a Windows 7 64-bit machine with an Intel W3580 CPU with 12 GB of RAM. This means that heart rate and heartbeat temporal locations can be computed approximately four times every second, with an initial 8-s delay.

References

1. Akay M (1998) Time frequency and wavelets in biomedical signal processing. IEEE Press, Piscataway
2. Bakhtiari S, Elmer TW, Cox NM, Gopalsami N, Raptis AC, Liao S, Mikhelson I, Sahakian AV (2012) Compact millimeter-wave sensor for remote monitoring of vital signs. IEEE Trans Instrum Meas 61(3):830–841 doi:10.1109/TIM.2011.2171589
3. Droitcour AD (2006) Non-contact measurement of heart and respiration rates with a single-chip microwave doppler radar. PhD thesis, Stanford University
4. Geisheimer J, Greneker III EF (2001) A non-contact lie detector using radar vital signs monitor (RVSM) technology. IEEE Aerosp Electron Syst Mag 16(8):10–14
5. Jianqi W, Chongxun Z, Guohua L, Xijing J (2007) A new method for identifying the life parameters via radar. EURASIP J Appl Signal Process 2007(1):16–16
6. Lin JC (1992) Microwave sensing of physiological movement and volume change: a review. Bioelectromagnetics 13(6):557–565
7. Lubecke VM, Boric-Lubecke O, Host-Madsen A, Fathy AE (2007) Through-the-wall radar life detection and monitoring. In: Microwave Symposium. IEEE/MTT-S International, pp 769–772. IEEE
8. Lubecke OB, Ong PW, Lubecke VM (2002) 10 GHz Doppler radar sensing of respiration and heart movement. In: Bioengineering Conference, 2002. Proceedings of the IEEE 28th Annual Northeast, pp 55–56. IEEE
9. MATLAB: version 7.10.0 (2010) The MathWorks Inc., Natick, Massachusetts
10. Mikhelson IV, Bakhtiari S, Elmer II TW, Sahakian AV (2011) Remote sensing of heart rate and patterns of respiration on a stationary subject using 94-GHz millimeter-wave interferometry. IEEE Trans Biomed Eng 58(6):1671–1677. doi:10.1109/TBME.2011.2111371
11. Morgan DR, Zierdt MG (2009) Novel signal processing techniques for doppler radar cardiopulmonary sensing. Signal Process 89(1):45–66
12. Obeid D, Sadek S, Zaharia G, Zein GE (2009) Noncontact heartbeat detection at 2.4, 5.8, and 60 GHz: a comparative study. Microw Opt Technol Lett 51(3):666–669
13. Pan J, Tompkins WJ (1985) A real-time QRS detection algorithm. IEEE Trans Biomed Eng 3:230–236
14. Petkie DT, Benton C, Bryan E (2009) Millimeter wave radar for remote measurement of vital signs. In: Radar Conference, 2009 IEEE, pp 1–3. IEEE
15. Poor HV (1994) An introduction to signal detection and estimation. Springer, Berlin
16. Rioul, O, Vetterli, M (1991) Wavelets and signal processing. IEEE Signal Process Mag 8(4):14–38
17. Uenoyama M, Matsui T, Yamada K, Suzuki S, Takase B, Suzuki S, Ishihara M, Kawakami M (2006) Non-contact respiratory monitoring system using a ceiling-attached microwave antenna. Med Biol Eng Comput 44(9):835–840